IBRO Neuroscience Reports 12 (2022) 108–120

Contents lists available at ScienceDirect

IBRO Neuroscience Reports

journal homepage: www.sciencedirect.com/journal/IBRO-Neuroscience-Reports

Research paper

# Multifaceted roles of orexin neurons in mediating methamphetamine-induced changes in body temperature and heart rate

Kohei Miyata [a], Yoko Ikoma [a], Koshi Murata [b], Ikue Kusumoto-Yoshida [a], Kenta Kobayashi [d], Tomoyuki Kuwaki [a], Youichirou Ootsuka [a,c,*]

[a] Department of Physiology, Graduate School of Medical and Dental Sciences, Kagoshima University, Kagoshima, Japan
[b] Division of Brain Structure and Function, Faculty of Medical Sciences, University of Fukui, Fukui, Japan
[c] Flinders Health and Medical Research Institute, Discipline of Human Physiology, College of Medicine and Public Health, Flinders University, South Australia, Australia
[d] Section of Viral Vector Development, National Institute for Physiological Sciences, Aichi, Japan

ARTICLE INFO

*Keywords:*
Orexin
Glutamate
Thermoregulation
Autonomic function
Transgenic mice

ABSTRACT

Methamphetamine (METH), which is used to improve the alertness of narcoleptic patients, elicits autonomic physiological responses such as increases in body temperature, blood pressure and heart rate. We have shown that orexin synthesizing neurons, which have an important role in maintaining wakefulness, greatly contribute to the regulation of cardiovascular and thermoregulatory function. This regulation is partly mediated by glutamatergic as well as orexinergic signalling from the orexin neurons. These signals may also be involved in the autonomic response elicited by METH. This study aimed to determine if loss of either orexin or glutamate in orexin neurons would affect METH-induced changes in heart rate and body temperature. We used transgenic mice in which the vesicular glutamate transporter 2 gene was disrupted selectively in orexin-producing neurons (ORX;vGT2-KO), prepro-orexin knockout mice (ORX-KO), and control wild type mice (WT). We measured body temperature, heart rate and locomotor activity with a pre-implanted telemetry probe and compared the effect of METH (0.5, 2 and 5 mg/kg i.p.) on these parameters between these three groups. A low dose of METH induced hyperthermia and tachycardia responses in ORX;vGT2-KO mice, which were significant compared to ORX-KO and WT mice. The highest dose of METH induced hypothermia and bradycardia in ORX-KO mice, however, it induced hyperthermia in both WT and ORX;vGT2-KO mice. These results suggest that glutamate and orexin from orexin neurons have differential roles in mediating METH-induced changes in body temperature and heart rate.

## 1. Introduction

Methamphetamine (METH) and its derivatives are powerful psychostimulant drugs that increase arousal, alertness and lead to euphoria. METH also causes hyperactivity and complex physiological responses including an increase in body temperature (Namiki et al., 2005; Phelps et al., 2010; Polesskaya et al., 2011; Rusyniak et al., 2012; Yoshida et al., 1993). METH-induced hyperthermia, which occurs in both human and experimental animals, is sometimes life threating and can be fatal. Therefore, it is important to understand the mechanism underlying this hyperthermia. METH-induced hyperthermia and tachycardia are prevented by inhibition of neurons in the dorsomedial hypothalamus (Rusyniak et al., 2008), which plays an essential role in thermoregulatory and cardiovascular responses to physiological and emotional stimuli (DiMicco et al., 2006; Dimicco and Zaretsky, 2007; Kataoka et al., 2014; Kataoka et al., 2020). This indicates that METH-induced autonomic responses are mediated via its central and not peripheral action. However, the brain mechanisms involved are still largely unknown.

Orexins, also known as hypocretins, are neuropeptides that are produced exclusively by neurons in the perifornical-lateral hypothalamic area. Orexin-producing neurons have been demonstrated to play an important role in maintaining arousal (Sakurai, 2007). They also have a pivotal role in controlling autonomic functions including thermoregulatory and cardiovascular systems (Kuwaki, 2015; Kuwaki and Zhang, 2012; Zhang et al., 2006). Orexin neurons are activated by METH

*Abbreviation:* METH, methamphetamine; vGLUT2, vascular glutamate transporter-2.

* Correspondence to: Flinders Health and Medical Research Institute, Discipline of Human Physiology, College of Medicine and Public Health, Flinders University GPO Box 2100, Adelaide, SA 5001, Australia.
*E-mail address:* youichirou.ootsuka@flinders.edu.au (Y. Ootsuka).

https://doi.org/10.1016/j.ibneur.2022.01.002
Received 12 August 2021; Received in revised form 12 January 2022; Accepted 17 January 2022
Available online 19 January 2022

treatment (Estabrooke et al., 2001). Indeed, systemic administration of orexin receptor antagonists attenuates METH-induced hyperthermia and pressor responses (Behrouzvaziri et al., 2015; Rusyniak et al., 2012). Further, loss of orexin peptide by disruption of the orexin gene attenuates METH-induced hyperactivity (Mori et al., 2010). These lines of evidence suggest that orexin neurons are involved in the central mechanisms of METH-induced autonomic responses.

Orexin-expressing neurons also contain other neurotransmitters/modulators, including glutamate (Torrealba et al., 2003; Tsujino and Sakurai, 2009). We have shown that thermogenic responses to febrile and emotional interventions are attenuated in orexin neuron-ablated mice but not in prepro-orexin knockout mice that can still release other neurotransmitters (Takahashi et al., 2013; Zhang et al., 2010). We have also demonstrated that the aforementioned thermogenic responses are attenuated by glutamate antagonists, but not orexin receptor antagonists (Takahashi et al., 2013). These findings suggest that other co-transmitters from orexin neurons are responsible for the thermogenic responses. The most likely co-transmitter for this is glutamate, which is co-localized in orexin neurons and may also be involved in METH-induced autonomic responses.

Glutamate is taken up into synaptic vesicles by vesicular glutamate transporters before being released from the cell (El Mestikawy et al., 2011). Orexin neurons express predominantly vesicular glutamate transporter-2 (vGLUT2) (Rosin et al., 2003). In the present study, we created a transgenic line that selectively induced vGLUT2 deficiency in orexin-expressing neurons (Orexin-Cre;Vglut2$^{flox/flox}$) by crossing Orexin-Cre mice, in which orexin neurons express Cre-recombinase (Matsuki et al., 2009), with Vglut2 $^{flox/flox}$ mice, wherein exon 2 of Vglut2 gene is flanked by LoxP sites (Tong et al., 2007). We also used prepro-orexin knockout mice (Chemelli et al., 1999) and wild type mice, comparing METH-induced changes to body temperature and heart rate between these three mice groups.

## 2. Material and methods

All experiments except in situ hybridisation was conducted at Kagoshima University. The in situ hybridisation was conducted at the University of Fukui. All procedures were approved by the Institutional Animal Care and Use Committee of both universities. The number of animals used and their suffering was minimized as much as possible.

### 2.1. Animals

Two types of genetically modified mice (ORX-KO, male, n = 9, 28.8 – 46.1 g and Orexin-Cre;Vglut2$^{flox/flox}$, n = 12, 26.1 – 36.1 g) and control wild type mice (WT) (C57BL/6, male, $n$ = 9, 27.7 – 43.1 g) were used. Orexin-Cre;Vglut2$^{flox/flox}$ mice (hereafter called ORX;vGT2-KO) were obtained by crossing orexin-Cre mice (Matsuki et al., 2009) with Vglut2$^{flox/flox}$ mice (Tong et al., 2007). The prepro-orexin knock out mice (hereafter called ORX-KO)(Chemelli et al., 1999) and orexin-Cre mice (Matsuki et al., 2009) were provided by Dr. Takeshi Sakurai (Tsukuba University). Vglut2$^{flox/flox}$ mice were provided by Dr. Bradford Lowell (Beth Israel Deaconess Medical Center and Harvard Medical School). The genotype of ORX-KO mice was identified using polymerase chain reaction (PCR) of extracted DNA (Kayaba et al., 2003). For genotyping ORX;vGT2-KO mice, we used 5′ primer, GTC TAC TGT AAG TGA AGA CAC and 3′ primer, CTT TAG GCT TTC ATC CTT GAG for a loxP site in intron 1 and another 5′ primer, CCT GAG CGA AGG TGA GCT GAA with a 3′ primer CCA AAT ACC TGA AAG TTA CTG to identify another loxP site in intron 2.

### 2.2. Surgery

Under inhalation anaesthesia (0.5 ml/min, 2–3%) of isoflurane (Escain inhalation anaesthetics, Mylan Inc., Pennsylvania, USA), mice were surgically implanted with a telemetry probe (ETA-F10, Data Science International Inc., MN, USA) that transmits electrocardiograms (ECG) and body temperature. During surgery, body temperature was maintained on a heat pad. At the end of surgery, mice were given a hypodermic injection of antibiotics (penicillin, 8 mg/ml, Nacalai Tesque, Kyoto, Japan). Following surgery, mice were individually caged and allowed to recover for at least one week in a quiet environment with ad libitum access to food and water.

### 2.3. Experimental procedures

All recordings were performed at an ambient temperature between 25 and 28 ℃ in a sound-insulated recording room with a 12-hour light-dark cycle (lights on at 0700). The experimental mouse was transferred to the recording room at least 36 h prior to any recording as a habituation period. During the experimental recording and habituation periods, the mouse received ad libitum access to food and water.

Recordings started at 14:00 on the day before METH treatment and stopped at 14:00 on the day after treatment. At 10:00 on treatment day, 0.5, 2.0 or 5.0 mg/kg of METH (methamphetamine hydrochloride, Sumitomo Dainippon Pharma, Tokyo, Japan), or 0.9% saline (0.4 ml), was injected intraperitoneally. Mice received these METH treatments in a counterbalanced rotating order to avoid serial effects with at least a 5-day recovery period between each injection. When a mouse had to be euthanized due to misadventure, the mouse was replaced with a new one.

### 2.4. Data recording and analysis

The amount of locomotor activity was measured using infrared-light-beams (XY grid pattern, 5 cm apart, homebuilt). This measuring instrument outputs an analogue block pulse (4 V, 170 msec/detection) when a mouse interrupts the infrared beam. Body temperature and ECG were measured with a pre-implanted telemetry probe. Ambient temperature in the experimental room was measured with a thermometer (BW-T100, Bio Research Center Co., Ltd, Nagoya, Japan). All measured signals were digitalized (400 Hz for ECG, 1 Hz for body temperature, 100 Hz for locomotor activity, and 1 Hz for room temperature) with PowerLab/16S (ADInstruments, NSW, Australia) and captured with Chart software (ADInstruments). The captured signals were analysed with Igor Pro (WaveMetrics, Inc., OR, USA). When signals were lost due to noise disturbance, values were interpolated with values at surrounding time points. Heart rate was calculated from an R-R interval in the ECG. The pulse signals of locomotor activity were integrated every 60 s. The mean value during 20 min pre-injection period (time −30 to −10 min before administration) was calculated as the pre-injection reference value.

### 2.5. Virus injections

Vglut2$^{flox/flox}$ mice were anesthetized with Ketamine (80 mg/kg) and Xylazine (20 mg/kg), and placed in a stereotaxic head frame (Narishige). A 30-gauge bevelled metal needle connected via a tube to a microsyringe pump (Pump11 Elite, Harvard Apparatus) was used to infuse a viral vector at a rate of 100 nl per min. After infusion, the needle was kept in the injection site for 5 min and then slowly withdrawn. AAV5-CMV-GFP-Cre ($7.8 \times 10^{10}$ vg/ml) were injected in the lateral hypothalamus (LH) (anterior-posterior (AP) 1.9, lateral (L) 1.0, ventral (V) 5.0–5.5 mm) with 0.5 μl per injection site. The plasmid for AAV production of (AAV-GFP/Cre) was gifted by Dr. Fred Gage (Addgene plasmid # 49056; http://n2t.net/addgene:49056; RRID:Addgene_49056) (Kaspar et al., 2002). The AAV vector was prepared as described previously (Kobayashi et al., 2016). After four weeks recovery period, the mice were used as part of the in situ hybridization examinations.

### 2.6. RNA probe preparation for in situ hybridization

To confirm deficiency of the Vglut2 gene in orexin neurons, we performed fluorescent labelling of mRNA for Vglut2 exon2 or of orexin using digoxigenin (DIG)-labelled RNA probes and immunoreactivity against orexin as described previously with modification (Watakabe et al., 2010). cDNAs for mouse Vglut2 exon 2 and orexin were sub-cloned by conventional PCR with commercial cDNA library (MD-01, Genostaff) and the following primer sets: Vglut2 exon 2, ggtgctggagaagaagcag – ctccttgataactttgcctccg; Orexin, ttccttctacaaaggttccctg – caggacaaggatagaagatggg. These sub-cloned cDNAs were inserted into vectors (pGEM®-T easy vector, Promega). We prepared DIG-labelled RNA probes with Roche's in vitro transcription kit (11277073910, Roche).

### 2.7. In situ hybridization

AAV-injected mice were euthanatized with an overdose of urethane, and perfused with 0.01 M phosphate buffered saline (PBS) and then 4% paraformaldehyde. The brain was removed and immersed in 4% paraformaldehyde for 1 night and then 30% sucrose for 2 nights. It was then immersed in water-soluble glycols and resin-based embedding medium (OCT compound, Sakura Finetek) and frozen at − 80 °C. The brain was sliced into coronal sections, of 20 μm thickness, using a cryotome. The sections were rinsed in PBS and 0.1 M PB, mounted on glass slides (CREST coat, Matsunami) and dried overnight in a vacuum desiccator. They were then stored at 4 °C until immunohistochemical analysis.

In situ hybridization was performed as described previously (Murata et al., 2020). Dried sections were fixed in 4% paraformaldehyde, digested with Proteinase K (10 μg/ml) for 30 min and then post-fixed in 4% paraformaldehyde again to deactivate this proteinase. Sections were then incubated overnight at 65 °C with DIG-labelled RNA probes. After stringent washing, the sections were incubated in 1% blocking buffer (11096176001, Roche) for 1 h and then in goat anti-orexin antibody (1:400 dilution, sc-8070, Santa Cruz) and anti-DIG antibody conjugated with alkaline phosphatase (1:500 dilution, Roche) overnight. After incubation, the sections were washed three times in Tris-NaCl-Tween buffer (TNT) (0.1 M Tris-HCl, pH 7.5, 0.15 M NaCl, 0.1% Tween 20). Following this, they were incubated with Alexa Fluor 488-conjugated secondary antibody (1:400 dilution, Jackson ImmunoResearch) for 2 h, washed three times in TNT and once in Tris buffer (0.1 M Tris-HCl, pH 8.0, 0.1 M NaCl, 50 mM MgCl2). Further incubation with a fluorescent substrate for alkaline phosphatase (HNPP fluorescence detection set, 11758888001, Roche) was also performed. This incubation was carried out for 30 min, repeated a total of 3 times, and stopped by washing in PBS. Sections were then counterstained with DAPI diluted in PBS (2 μg/ml) for 5 min. After washing in PBS, sections were mounted on slides with aqueous mounting medium (PermaFluor, Thermo Fisher Scientific). Examination was done with a confocal laser microscope (FV1200, Olympus) for localization of mRNA signals.

### 2.8. Statistical procedures

Statistical analysis was performed using SPSS (IBM Corp., Armonk, NY, USA). Group data were shown as mean±SEM. Pre- and post-injection values were compared using a paired t-test. Data between doses in wild type animals, or between genotypes at each dose were analysed using one-way factorial ANOVA. If the primary analysis showed significant, a post-hoc analysis was performed using Fisher's least significant difference test. The significance threshold was set at 0.05 level. Regression analysis (linear regression of log-dose) was used to determine dose-response relationships.

## 3. Results

### 3.1. Effect of methamphetamine on body temperature, heart rate and locomotor activity in WT mice

After injection of vehicle, body temperature transiently increased from 34.7 ± 0.5 ℃ to 36.3 ± 0.3 ℃ ($P = 0.00061$, paired t-test, $n = 7$) and peaked within 20 min (Fig. 1). Similarly to the body temperature response, heart rate increased from 479 ± 20 bpm to 659 ± 15 bpm ($P = 0.00066$, paired t-test, $n = 7$) and peaked within 5 min. Locomotor activity also increased from 37 ± 24–228 ± 61 (arbitrary unit) ($P = 0.0099$, paired t-test, $n = 7$).

METH (0.5, 2.0 and 5.0 mg/kg) caused a similar transient increase in body temperature and heart rate. After the initial increase, body temperature changed again, and its pattern was different between the three doses. At a low dose of METH, body temperature gradually deceased to pre-injection level. At the middle and highest doses, body temperature decreased towards pre-injection level, then increased and peaked at ~200 min after injection (Fig. 1a). The mean increase in body temperature during the 300 min post-injection observation period for the highest dose was significantly larger compared to other treatments ($F_{(3,25)} = 4.554$, $P = 0.011$, ANOVA; post-hoc, $P = 0.015$ for 5.0 mg/kg vs vehicle, $P = 0.002$ for 5.0 mg/kg vs 0.5 mg/kg)(Fig. 1d). The effect of METH on heart rate was variable depending on dose. At the low and middle dose, heart rate decreased after the initial transient increase. At the highest dose, heart rate decreased and then increased. Overall, however, changes in heart rate during the 300 min post-injection period were not significant between the four treatments ($F_{(3,25)} = 0.899$, $P = 0.445$, ANOVA) (Fig. 1e). ANOVA analysis between doses showed significant effects of METH on locomotor activity ($F_{(3,25)} = 14.1333$, $P = 0.000014$; post-hoc, $P = 0.000006$ for 5.0 mg/kg vs vehicle, $P = 0.000015$ for 5.0 mg/kg vs 0.5 mg/kg, $P = 0.009$ for 5.0 mg/kg vs 2.0 mg/kg) and METH increased locomotor activity in a dose-dependent manner ($F_{(1,20)} = 22.946$ $P = 0.000112$, $R^2 = 0.534$ log-dose linear regression). At the highest dose, locomotor responses to METH were bimodal with the 1st peak at ~60 min and the second peak at ~160 min (Fig. 1c).

Since body temperature and locomotor activity responses had two phases, we divided the 300 min post-injection period into two parts; the first phase (0–100 min) and the second phase (100–300 min) for further analysis (Fig. 1). In the first phase, METH-induced increases in locomotor activity for the middle and the high dose of METH were significantly larger when compared to vehicle and that low dose of METH ($F_{(3,25)} = 11.977$, $P = 0.000047$, ANOVA; post-hoc, $P = 0.000149$ for 2.0 mg/kg vs 0.5 mg/kg, $P = 0.000065$ for 5.0 mg/kg vs 0.5 mg/kg). The effect of METH on body temperature and heart rate was not different between doses ($F_{(3,25)} = 0.253$, $P = 0.858$ for body temperature, $F_{(3,25)} = 1.338$, $P = 0.284$ for heart rate, ANOVA). In the second phase, METH-induced increases in body temperature and locomotor activity were significantly larger for the middle and high dose of METH compared to vehicle and low dose of METH ($F_{(3,25)} = 8.469$, $P = 0.000471$ for body temperature, ANOVA; post-hoc, $P = 0.036$ for 2.0 mg/kg vs 0.5 mg/kg, $P = 0.019$ for 2.0 mg/kg vs 5.0 mg/kg, $P = 0.001$ for 5.0 mg/kg vs vehicle, $P = 0.000064$ for 5.0 mg/kg vs 0.5 mg/kg)($F_{(3,25)} = 14.766$, $P = 0.00001$ for locomotor activity, ANOVA; post-hoc, $P = 0.000009$ for 5.0 mg/kg vs vehicle in 2nd phase, $P = 0.000006$ for 5.0 mg/kg vs 0.5 mg/kg in 2nd phase, $P = 0.000164$ for 5.0 mg/kg vs 2.0 mg/kg in 2nd phase). The effect of METH on heart rate was not different between doses ($F_{(3,25)} = 1.888$, $P = 0.157$, ANOVA).

### 3.2. Comparing effect of methamphetamine on body temperature between WT, ORX-KO and ORX;vGT2-KO mice

After vehicle injection, body temperature increased in ORX-KO and ORX;vGT2-KO mice and returned to the pre-injection level in the first

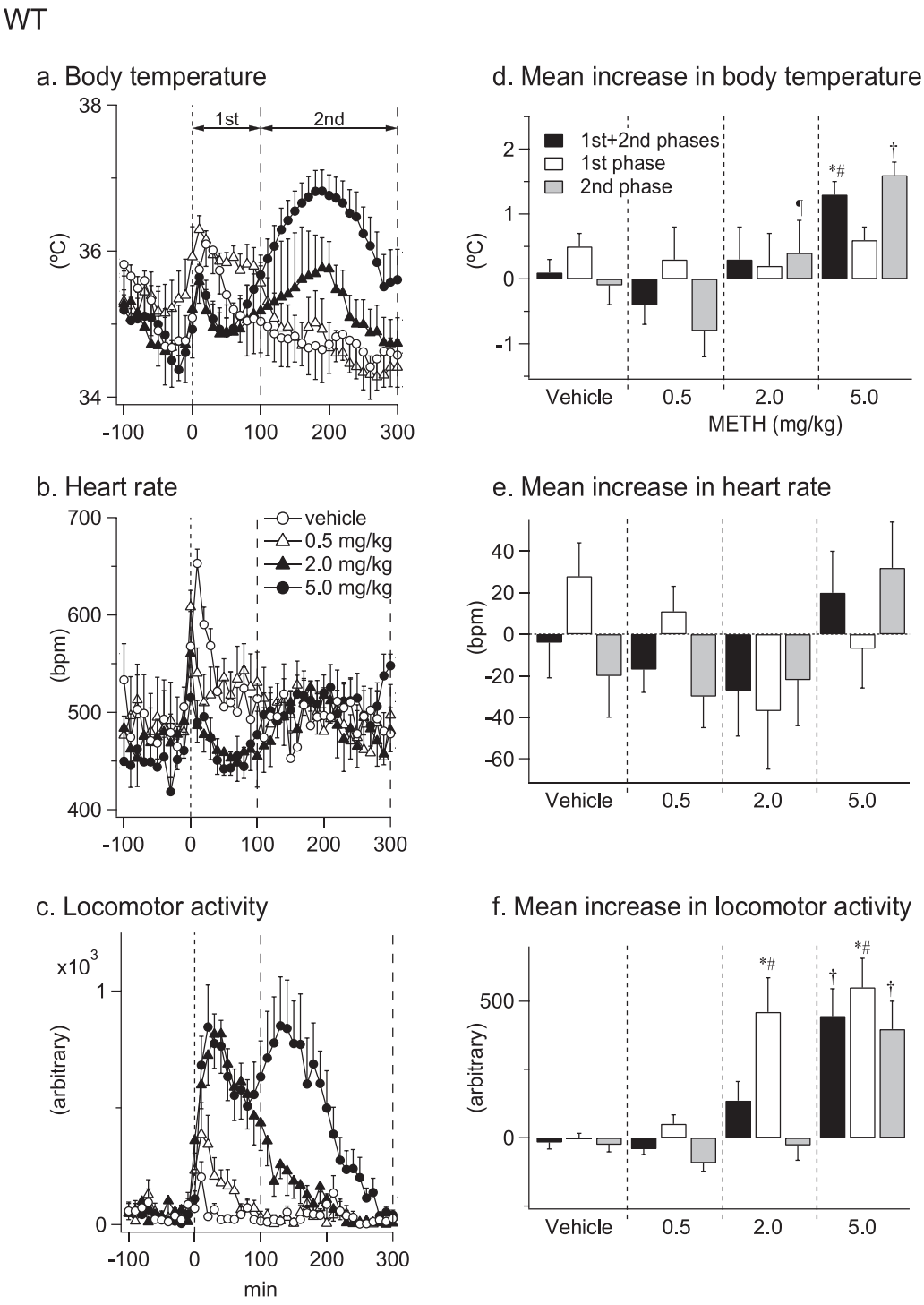


**Fig. 1.** The effect of METH on recorded physiological parameters in wild type (WT) mice. Left graphs show changes (10 min means) of body temperature (a), heart rate (b) and body temperature (c) in response to vehicle or METH injected at time 0 (n = 7 for vehicle, 0.5 and 2.0 mg/kg and n = 8 for 5.0 mg/kg). Right vertical bar graphs show mean changes in each parameter from pre-injection level during 0–300 min (1st+2nd phases), 0–100 min (1st phase) and 100–300 min (2nd phase) after injection. ANOVA analysis between doses shows significant effects of METH on body temperature (d) ($F_{(3,25)}$= 4.554, P = 0.011 for 1st+ 2nd phases, $F_{(3,25)}$= 0.253, P = 0.858 for 1st phase, $F_{(3,25)}$= 8.469, P = 0.000471 for 2nd phase) and locomotor activity (f) ($F_{(3,25)}$= 14.133, P = 0.000014 for 1st+ 2nd phases, $F_{(3,25)}$= 11.977, P = 0.000047 for 1st phase and $F_{(3,25)}$= 14.766, P = 0.00001 for 2nd phase), but not on heart rate (e) ($F_{(3,25)}$= 0.899, P = 0.455 for 1st+ 2nd phases, $F_{(3,25)}$= 1.338, P = 0.284 for 1st phase and $F_{(3,25)}$= 1.888, P = 0.157 for 2nd phase). * a significant difference compared to vehicle (post-hoc after ANOVA) (body temperature, P = 0.015 for 5.0 mg/kg vs vehicle mg/kg in 1st+2nd phase; locomotor activity, P = 0.000149 for 2.0 mg/kg vs 0.5 mg/kg in 1st phase, P = 0.000065 for 5.0 mg/kg vs 0.5 mg/kg in 1st phase). # a significant difference compared to 0.5 mg/kg (post-hoc after ANOVA) (body temperature: P = 0.002 for 5.0 mg/kg vs 0.5 mg/kg in 1st+2nd phase). ¶ a significant difference compared to other METH treatments (post-hoc after ANOVA) (body temperature, P = 0.036 for 2.0 mg/kg vs 0.5 mg/kg in 2nd phase, P = 0.019 for 2.0 mg/kg vs 5.0 mg/kg in 2nd phase). † a significant difference compared to other METH treatments and vehicle (post-hoc after ANOVA) (body temperature, P = 0.001 for 5.0 mg/kg vs vehicle, P = 0.000064 for 5.0 mg/kg vs 0.5 mg/kg in 2nd phase, P = 0.019 for 5.0 mg/kg vs 2.0 mg/kg in 2nd phase; locomotor activity, P = 0.000006 for 5.0 mg/kg vs vehicle in 1st+2nd phase, P = 0.000015 for 5.0 mg/kg vs 0.5 mg/kg in 1st+2nd phase, P = 0.009 for 5.0 mg/kg vs 2.0 mg/kg in 1st+2nd phase, P = 0.000009 for 5.0 mg/kg vs vehicle in 2nd phase, P = 0.000006 for 5.0 mg/kg vs 0.5 mg/kg in 2nd phase, P = 0.000164 for 5.0 mg/kg vs 2.0 mg/kg in 2nd phase,). Group data are expressed as mean±SEM.

phase similar to WT mice (Fig. 2a). Mean temperature increase during the first phase was not significantly different between the three genetic groups ($F_{(2,21)}$= 1.207, P = 0.319).

As with vehicle treatment, there was an initial increase in body temperature following METH treatment. After the initial increase, body temperature changed again, and its pattern differed depending on dose and genotype.

At the low dose of METH (0.5 mg/kg), in ORX;vGT2-KO mice, body temperature was sustained at a high level during the first phase and then returned to the pre-injection level in the second phase (Fig. 2b). The mean increase during the first phase was 2.0 ± 0.4°C (n = 7), which was significantly larger than the corresponding values in WT (0.6 ± 0.3°C,

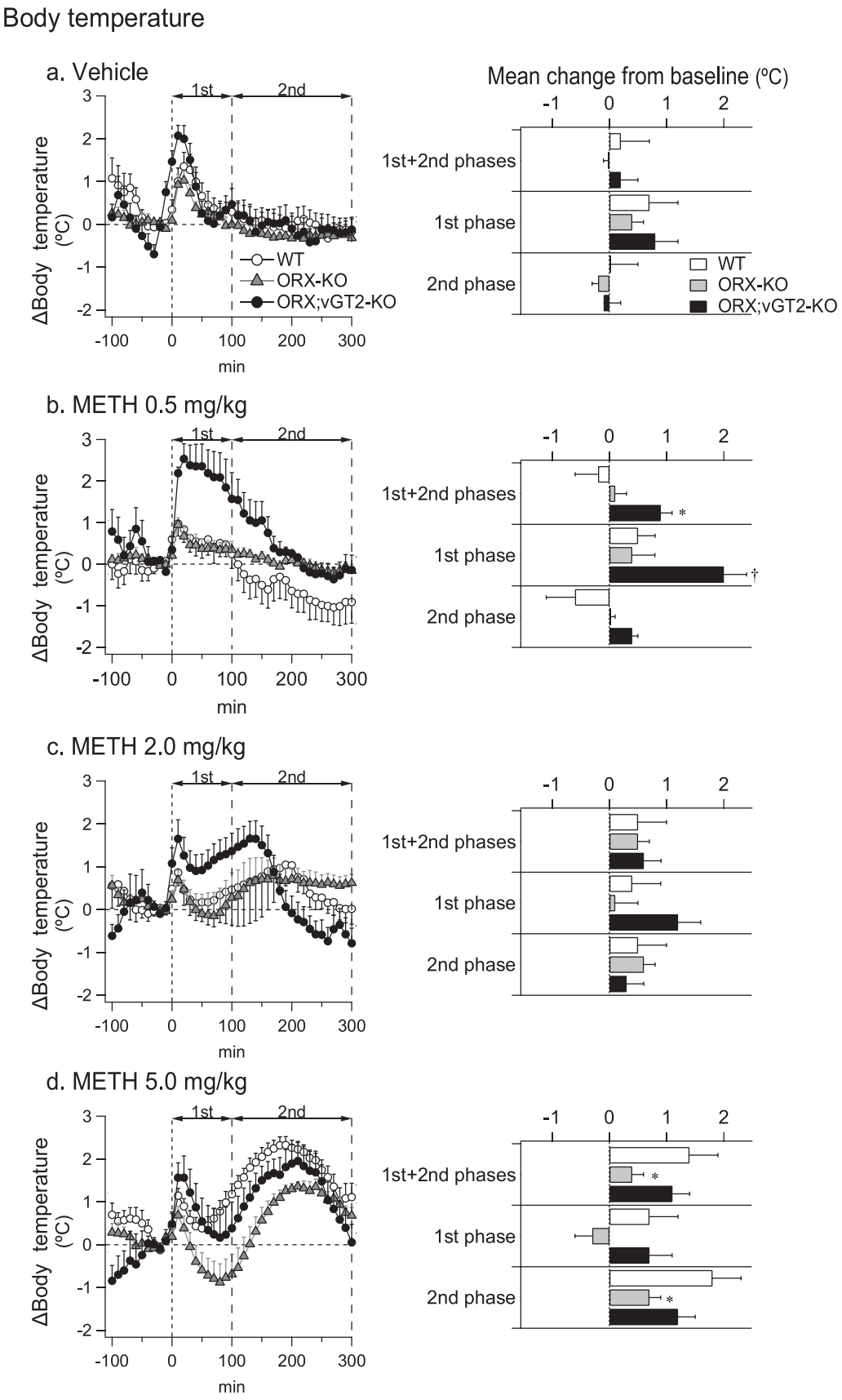


**Fig. 2.** The effect of METH on body temperature in WT, ORX-KO and ORX;vGT2 mice. Left graphs show changes (10 min means) of body temperature to vehicle (n = 7 for WT, n = 7 for ORX-KO, n = 10 for ORX;vGT2), METH 0.5 mg/kg (n = 7 for WT, n = 8 for ORX-KO, n = 7 for ORX;vGT2), METH 2.0 mg/kg (n = 7 for WT, n = 8 for ORX-KO, n = 9 for ORX;vGT2) and METH 5.0 mg/kg (n = 8 for WT, n = 7 for ORX-KO, n = 7 for ORX;vGT2) injected at time 0. Right horizontal bar graphs show mean changes in each parameter from pre-injection level during 0–300 min (1st+2nd phases), 0–100 min (1st phase) and 100–300 min (2nd phase) after the injection. ANOVA analysis between genotypes shows the significant effect of METH at 0.5 mg/kg ($F_{(2,19)}$= 4.625, P = 0.023 for 1st+ 2nd phases, $F_{(2,19)}$= 7.651, P = 0.004 for 1st phase, $F_{(2,19)}$= 3.262, P = 0.061 for 2nd phase) and 5.0 mg/kg ($F_{(2,19)}$= 4.377, P = 0.027 for 1st+ 2nd phases, $F_{(2,19)}$= 2.919, P = 0.078 for 1st phase, $F_{(2,19)}$= 5.148, P = 0.016 for 2nd phase) but not at 2.0 mg/kg ($F_{(2,21)}$= 0.046, P = 0.955 for 1st+ 2nd phases, $F_{(2,21)}$= 1.838, P = 0.184 for 1st phase, $F_{(2,21)}$= 0.189, P = 0.829 for 2nd phase) and vehicle ($F_{(2,21)}$= 0.422, P = 0.654 for 1st+ 2nd phases, $F_{(2,21)}$= 1.207, P = 0.319 for 1st phase, $F_{(2,21)}$= 0.219, P = 0.805 for 2nd phase). * a significant difference compared to WT (post-hoc after ANOVA) (0.5 mg/kg, P = 0.008 in for WT vs ORX;vGT2-KO in 1st+2nd phase, P = 0.005 for WT vs ORX;vGT2-KO in 1st phase; 5.0 mg/kg, P = 0.009 for WT vs ORX-KO in 1st+2nd phases, P = 0.005 for WT vs ORX-KO in 2nd phase at). † a significant difference compared to other genotypes (post-hoc after ANOVA) (0.5 mg/kg, P = 0.005 for ORX;vGT2-KO vs WT in 1st phase, P = 0.002 for ORX;vGT2-KO vs ORX-KO in 1st phase). Group data are expressed as mean±SEM.

n = 7) and ORX-KO mice (0.4 ± 0.2 ℃, n = 8) ($F_{(2,19)}$= 7.651, P = 0.004; post hoc P = 0.005 for ORX;vGT2-KO vs WT, P = 0.002 for ORX;vGT2-KO vs ORX-KO) (Fig. 2a). In ORX-KO mice, the mean increase during the first phase was similar to that for the vehicle control (P = 0.84). The mean changes during the second phase were not significantly different between these genotypes ($F_{(2,19)}$= 3.262, P = 0.061).

At a middle dose of METH (2.0 mg/kg), after the initial increase, body temperature decreased towards pre-injection level and then started increasing again during the first phase in ORX;vGT2-KO and ORX-KO mice (Fig. 2c). Mean changes in body temperature during the 300 min post-injection period and the first and second phases were similar between the three genotypes ($F_{(2,21)}$= 0.046, P = 0.955 for the 300 min, $F_{(2,21)}$= 1.838, P = 0.184 for 1st phase and $F_{(2,21)}$= 0.189, P = 0.829 for 2nd phase, ANOVA).

At the highest dose of METH (5.0 mg/kg), body temperature decreased towards pre-injection level in ORX;vGT2-KO mice after the initial increase seen during the first phase, as in WT controls (Fig. 2d). In ORX-KO mice, body temperature decreased below pre-injection level and reached the nadir at ~80 min after the injection (−1.0 ± 0.4 ℃, n = 7, P = 0.021, paired t-test). Mean changes during the first phase were not significantly difference between these genotypes ($F_{(2,19)}$= 2.919, P = 0.078). After the decrease, body temperature increased again and peaked during the second phase in all three genotypes. Mean temperature increase in the second phase for ORX-KO mice was significantly less compared to WT mice ($F_{(2,19)}$= 5.148, P = 0.016 ANOVA with post-hoc P = 0.005).

### 3.3. Comparing effect of METH on heart rate between WT, ORX-KO and ORX;vGT2-KO mice

Vehicle treatment caused a similar transient increase in heart rate during the first phase in ORX-KO and ORX;vGT2-KO mice, as also seen in WT mice ($F_{(2,21)}$= 0.132, P = 0.877, ANOVA)(Fig. 3a). Similar to the effect of METH on body temperature, METH-induced changes in heart rate after the initial tachycardia differed depending on dose and genotype.

At the low dose of METH (0.5 mg/kg), heart rate in ORX;vGT2-KO mice was kept above the pre-injection level during the first phase and then returned to pre-injection level during the second phase. Mean change in heart rate from pre-injection level during the first phase was significantly larger than for WT and ORX-KO mice ($F_{(2,19)}$= 8.593, P = 0.002, ANOVA; post-hoc, P = 0.006 for ORX;vGT2-KO vs WT, P = 0.001 for ORX;vGT2-KO vs ORX-KO)(Fig. 3b). Mean changes during the second phase were not significantly different between the genotypes ($F_{(2,19)}$= 1.866, P = 0.182). At the middle dose of METH (2.0 mg/kg), heart rate returned to pre-injection level during the first phase in all three genotypes (Fig. 3c). The mean change in heart rate during the first and second phases were similar between genotypes ($F_{(2,21)}$= 2.104, P = 0.147 for the first phase and $F_{(2,21)}$= 0.119, P = 0.888 for the second phase, ANOVA). At the highest dose of METH (5.0 mg/kg), heart rate decreased below pre-injection level after the initial tachycardia in ORX-KO and ORX;vGT2-KO mice and reached the minimum level during the first phase (Fig. 3d). These changes in heart rate were significantly different from what was seen in WT mice ($F_{(2,19)}$= 6.156, P = 0.009 for the first phase, ANOVA; post-hoc, P = 0.03 for WT vs ORX-KO, P = 0.033 for WT vs ORX;vGT2-KO). After this decrease, heart rate returned to the pre-injection level during the second phase in all genotypes ($F_{(2,19)}$= 2.824, P = 0.086).

### 3.4. Comparing effect of METH on locomotor activity between WT, ORX-KO and ORX;vGT2-KO mice

Similar to WT mice, METH caused a monophasic increase in locomotor activity at the middle dose (2.0 mg/kg) and a bimodal increase at the highest dose (5.0 mg/kg) in both ORX-KO and ORX;vGT2-KO mice. The mean increase during 0–300 min was does-dependent ($F_{(1,21)}$= 15.160, P = 0.001, $R^2$ = 0.39, log-dose linear regression for ORX-KO; $F_{(1,21)}$= 16.332, P = 0.001, $R^2$ = 0.41, log-dose linear regression for ORX;vGT2-KO). The regression slopes were not different between the three genotypes ($F_{(2,62)}$= 1.331, P = 0.272, ANOVA). ANOVA analysis between the genotypes showed that the effect of METH was significant only in the second phase at 0.5 mg/kg ($F_{(2,19)}$= 4.04, P = 0.035 for second phase; post-hoc, ORX-KO vs WT, P = 0.011) (Figs. 4b) and 2 mg/kg doses ($F_{(2,21)}$= 5.037, P = 0.016; post hoc, P = 0.01 for ORX-KO vs WT, P = 0.016 for ORX-KO vs ORX;vGT2-KO) (Fig. 4c), but not in other phases at any doses (0.5 mg/kg, $F_{(2,19)}$= 1.941, P = 0.171 for, $F_{(2,19)}$= 1.807, P = 0.191 for 1st phase; 2.0 mg/kg, $F_{(2,21)}$= 1.318, P = 0.289 for 1st+ 2nd phases, $F_{(2,21)}$= 1.221, P = 0.315 for 1st phase; 5.0 mg/kg, $F_{(2,19)}$= 1.214, P = 0.319 for 1st+ 2nd phases, $F_{(2,19)}$= 1.277, P = 0.302 for 1st phase, $F_{(2,19)}$= 0.234, P = 0.794 for 2nd phase; vehicle, $F_{(2,21)}$= 0.324, P = 0.727 for 1st+ 2nd phases, $F_{(2,21)}$= 0.217, P = 0.807 for 1st phase, $F_{(2,21)}$= 0.772, P = 0.475 for 2nd phase).

### 3.5. Confirmation of deficiency of Vglut 2 gene in orexin neurons

To test for deletion of Vglut2 in orexin neurons, we performed in situ hybridization with a labelled RNA probe correspondent to Vglut2 exon 2. In control $Vglut2^{flox/flox}$ mice, 86 out of 197 (44%) orexin neurons were Vglut2-positive and expressed Vglut2 mRNA in the cytoplasm (Figs. 5A-a and 5B-d). In ORX;VGT2-KO mice, 72 out of 157 (46%) orexin neurons were Vglut2-positive, and 70 of these 72 neurons (97%) abnormally expressed Vglut2 mRNA, which was condensed and found only in nuclei but not in the cytoplasm (Figs. 5A-b and 5B-h). Two out of 157 (1%) orexin neurons showed the normal Vglut2 mRNA signal in the cytoplasm. The normal signal was shown in non-orexin neurons in both $Vglut2^{flox/flox}$ mice and ORX;VGT2-KO mice (Fig. 5 C).

To confirm whether the abnormal expression of mRNA in nucleus was due to Cre-driven denaturing specific to the Vglut2 gene, we used $Vglut2^{flox/flox}$ mice, injected the viral vectors (AAV5-CMV-GFP-Cre) into the unilateral LH to drive Cre-dependent recombination in orexin neurons and conducted the same in situ hybridization. The intra-nuclear abnormal condensation of Vglut2 mRNA was found in the viral injected site (Figs. 6A-a and 6A-d) but not in the contralateral control site (Figs. 6A-e and 6A-h). We also used an RNA probe correspondent to the orexin gene and found that there was no abnormal condensation and localization of orexin mRNA in both sites (Fig. 6B). These results rule out non-selective recombination action of Cre.

## 4. Discussion

This study has characterized, for the first time, METH-induced responses in body temperature and heart rate in ORX-KO and ORX;vGT2-KO mice. Body temperature and heart rate were increased after METH injection in ORX;vGT2-KO mice compared to WT mice, whereas they were decreased in ORX-KO mice, although the response patterns varied with dose. These results suggest that the orexin peptide and glutamate released from orexin neurons have distinctive roles in mediating METH-induced changes in body temperature and heart rate.

There have been few reports measuring dose-dependent changes in body temperature with a low range of METH doses (0.5–5 mg/kg) in normal mice. Most reports have investigated METH toxicity, in which high concentrations of METH (>5 mg/kg) are administered a couple of times every 2–3 h (Anneken et al., 2018; Fantegrossi et al., 2008; Kaushal et al., 2011). Some METH dose-dependent studies in mice used a higher dose range still (2–20 mg/kg, 1–40 mg/kg or 5–95 mg/kg), and measured colonic temperature by insertion of a temperature probe every 15–30 min (Funahashi et al., 1990; Funahashi et al., 1988;Namiki et al., 2005). Since frequent handling stress may complicate body temperature response to METH, it is not appropriate to compare the previous data with the present results. In rats, there are some reports examining

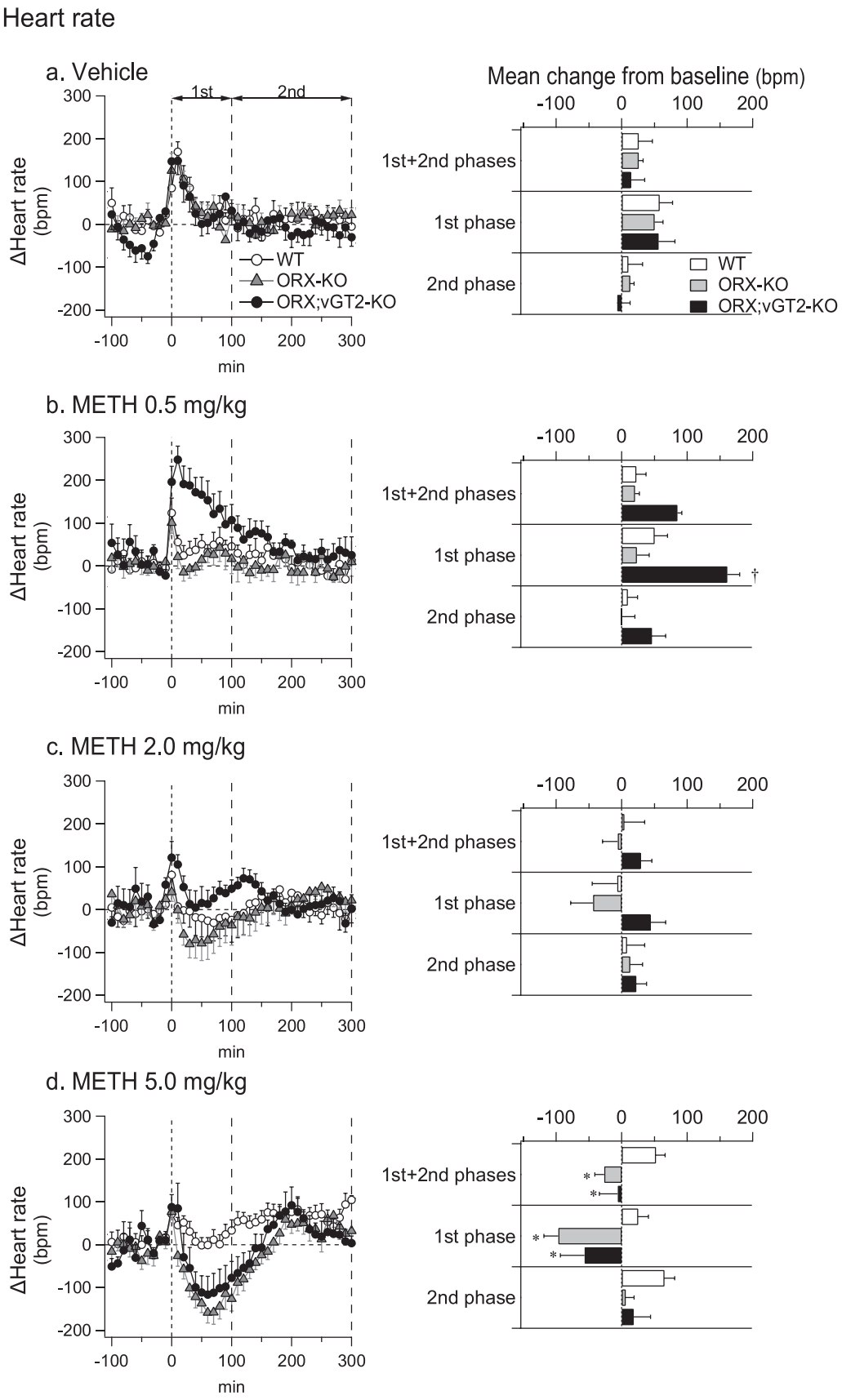


**Fig. 3.** The effect of METH on heart rate in WT, ORX-KO and ORX;vGT2 mice. Left graphs show changes (10 min means) of heart rate to vehicle (n = 7 for WT, n = 7 for ORX-KO, n = 10 for ORX;vGT2), METH 0.5 mg/kg (n = 7 for WT, n = 8 for ORX-KO, n = 7 for ORX;vGT2), METH 2.0 mg/kg (n = 7 for WT, n = 8 for ORX-KO, n = 9 for ORX;vGT2) and METH 5.0 mg/kg (n = 8 for WT, n = 7 for ORX-KO, n = 7 for ORX;vGT2) injected at time 0. Right horizontal bar graphs show mean changes in each parameter from pre-injection level during 0–300 min (1st+2nd phases), 0–100 min (1st phase) and 100–300 min (2nd phase) after the injection. ANOVA analysis between genotypes shows the significant effect of METH at 0.5 mg/kg ($F_{(2,19)}$= 4.698, P = 0.022 for 1st+ 2nd phases, $F_{(2,19)}$= 8.593, P = 0.002 for 1st phase, $F_{(2,19)}$= 1.866, P = 0.182 for 2nd phase) and 5.0 mg/kg ($F_{(2,19)}$= 4.507, P = 0.025 for 1st+ 2nd phases, $F_{(2,19)}$= 6.156, P = 0.009 for 1st phase, $F_{(2,19)}$= 2.824, P = 0.086 for 2nd phase) but not at 2.0 mg/kg ($F_{(2,21)}$= 0.651, P = 0.532 for 1st+ 2nd phases, $F_{(2,21)}$= 2.104, P = 0.147 for 1st phase, $F_{(2,21)}$= 0.119, P = 0.888 for 2nd phase) and vehicle ($F_{(2,21)}$= 0.132, P = 0.877 for 1st+ 2nd phases, $F_{(2,21)}$= 0.031, P = 0.970 for 1st phase, $F_{(2,21)}$= 0.348, P = 0.710 for 2nd phase). * a significant difference compared to WT (post-hoc after ANOVA) (5.0 mg/kg, P = 0.01 for WT vs ORX-KO in 1st+2nd phases, P = 0.048 for WT vs ORX;vGT2-KO in 1st+2nd phase, P = 0.03 for WT vs ORX-KO in 1st phases, P = 0.033 for WT vs ORX;vGT2-KO in 1st phase). † a significant difference compared to other genotypes (post-hoc after ANOVA) (0.5 mg/kg, P = 0.006 for ORX;vGT2-KO vs WT in 1st phase, P = 0.001 for ORX;vGT2-KO vs ORX-KO in 1st phase). Group data are expressed as mean±SEM.

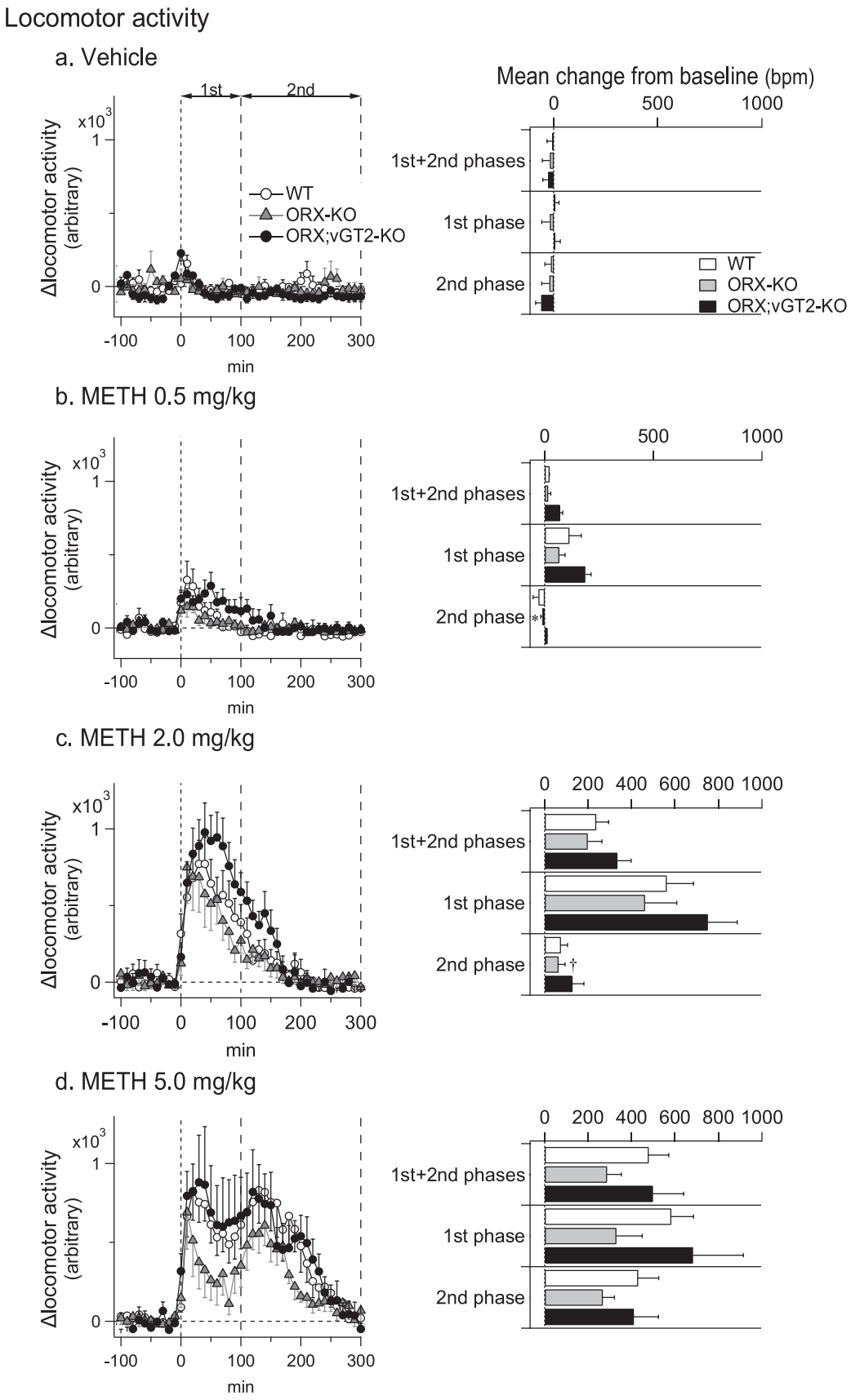


**Fig. 4.** The effect of METH on locomotor activity in WT, ORX-KO and ORX;vGT2 mice. Left show graphs changes (10 min means) of locomotor activity to vehicle (n = 7 for W, n = 7 for ORX-KO, n = 10 for ORX;vGT2), METH 0.5 mg/kg (n = 7 for WT, n = 8 for ORX-KO, n = 7 for ORX;vGT2), METH 2.0 mg/kg (n = 7 for WT, n = 8 for ORX-KO, n = 9 for ORX;vGT2) and METH 5.0 mg/kg (n = 8 for WT, n = 7 for ORX-KO, n = 7 for ORX;vGT2) injected at time 0. Right horizontal bar graphs show mean changes in each parameter from pre-injection level during 0–300 min (1st+2nd phases), 0–100 min (1st phase) and 100–300 min (2nd phase) after the injection. ANOVA analysis between genotypes shows the significant effect of METH in 2nd phase at 0.5 mg/kg ($F_{(2,19)}$= 4.04, P = 0.035 for 2nd phase) and 2 mg/kg ($F_{(2,21)}$= 5.037, P = 0.016) but not in other phases at any doses (0.5 mg/kg, $F_{(2,19)}$= 1.941, P = 0.171 for, $F_{(2,19)}$= 1.807, P = 0.191 for 1st phase; 2.0 mg/kg, $F_{(2,21)}$= 1.318, P = 0.289 for 1st+ 2nd phases, $F_{(2,21)}$= 1.221, P = 0.315 for 1st phase; 5.0 mg/kg, $F_{(2,19)}$= 1.214, P = 0.319 for 1st+ 2nd phases, $F_{(2,19)}$= 1.277, P = 0.302 for 1st phase, $F_{(2,19)}$= 0.234, P = 0.794 for 2nd phase; vehicle, $F_{(2,21)}$= 0.324, P = 0.727 for 1st+ 2nd phases, $F_{(2,21)}$= 0.217, P = 0.807 for 1st phase, $F_{(2,21)}$= 0.772, P = 0.475 for 2nd phase). * a significant difference compared to WT (post-hoc after ANOVA) (P = 0.011 in 2nd phase at 0.5 mg/kg). † a significant difference compared to other genotypes (post-hoc after ANOVA) (P = 0.01 for ORX-KO vs WT in 1st phase, P = 0.016 for ORX-KO vs ORX;vGT2-KO in 1st phase at 2.0 mg/kg). Group data are expressed as mean±SEM.

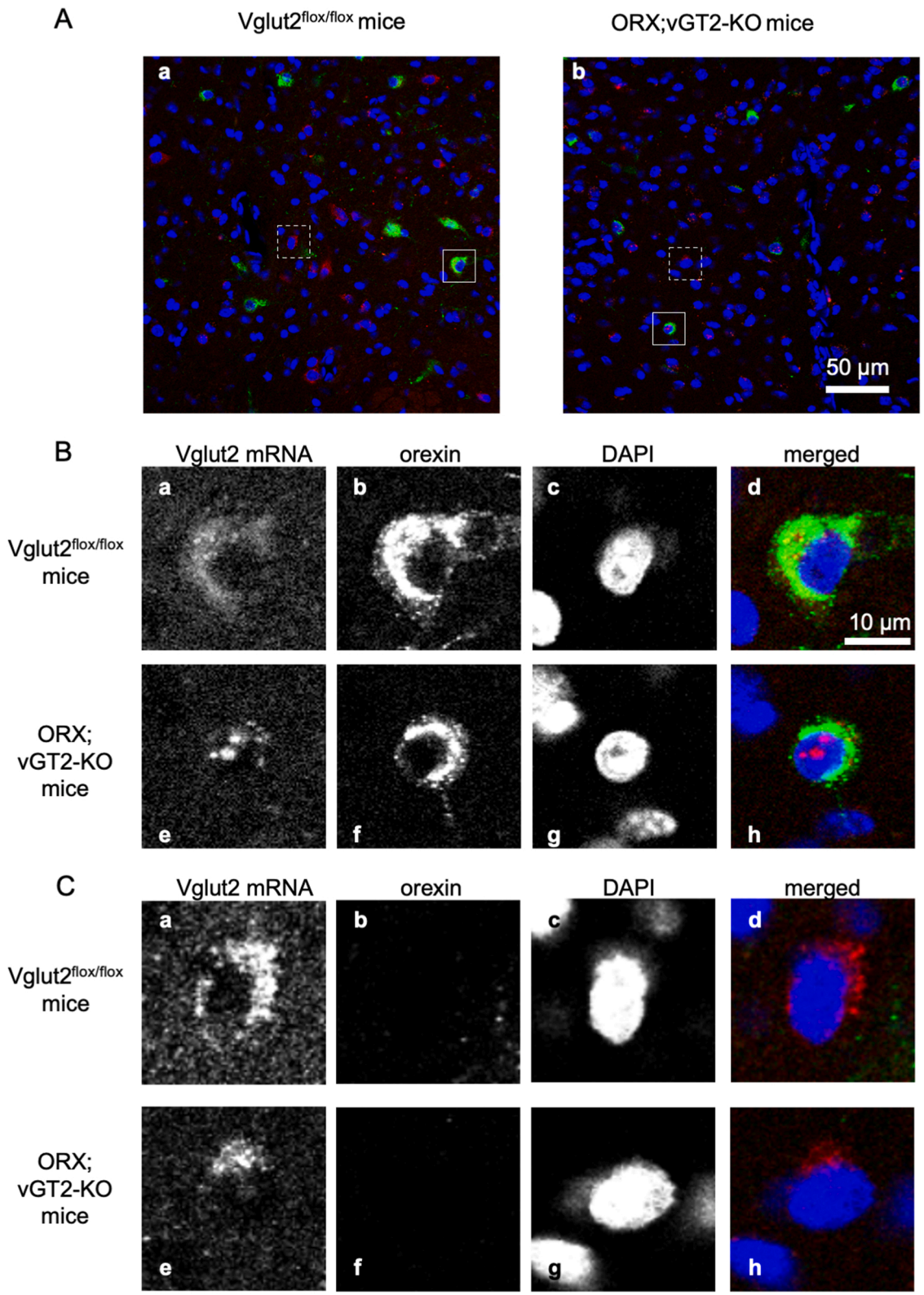


**Fig. 5.** Histochemical analysis showing deficiency of Vglut 2 gene in orexin neurons. A: Sections of the lateral hypothalamus from Vglut2$^{flox/flox}$ (a) and ORX;vGT2-KO mice (b) were stained for orexin (green), Vglut2 (red) and nuclei (blue). Orexin neurons (white box) and non-orexin neurons (dotted white box) were magnified in B and C, respectively. B: Normal Vglut2 mRNA expression (a and red in d) was found in cytoplasm (green in d) of the orexin neuron in Vglut2$^{flox/flox}$ mice, while abnormal condensation and localization of the mRNA (e and red in h) was found in the nucleus (blue in h) of orexin neurons in ORX;vGT2-KO mice. C: In both the control and experiment groups, normal Vglut2 mRNA expression was found in the non-orexin neurons. (For interpretation of the references to colour in this figure legend, the reader is referred to the web version of this article.)

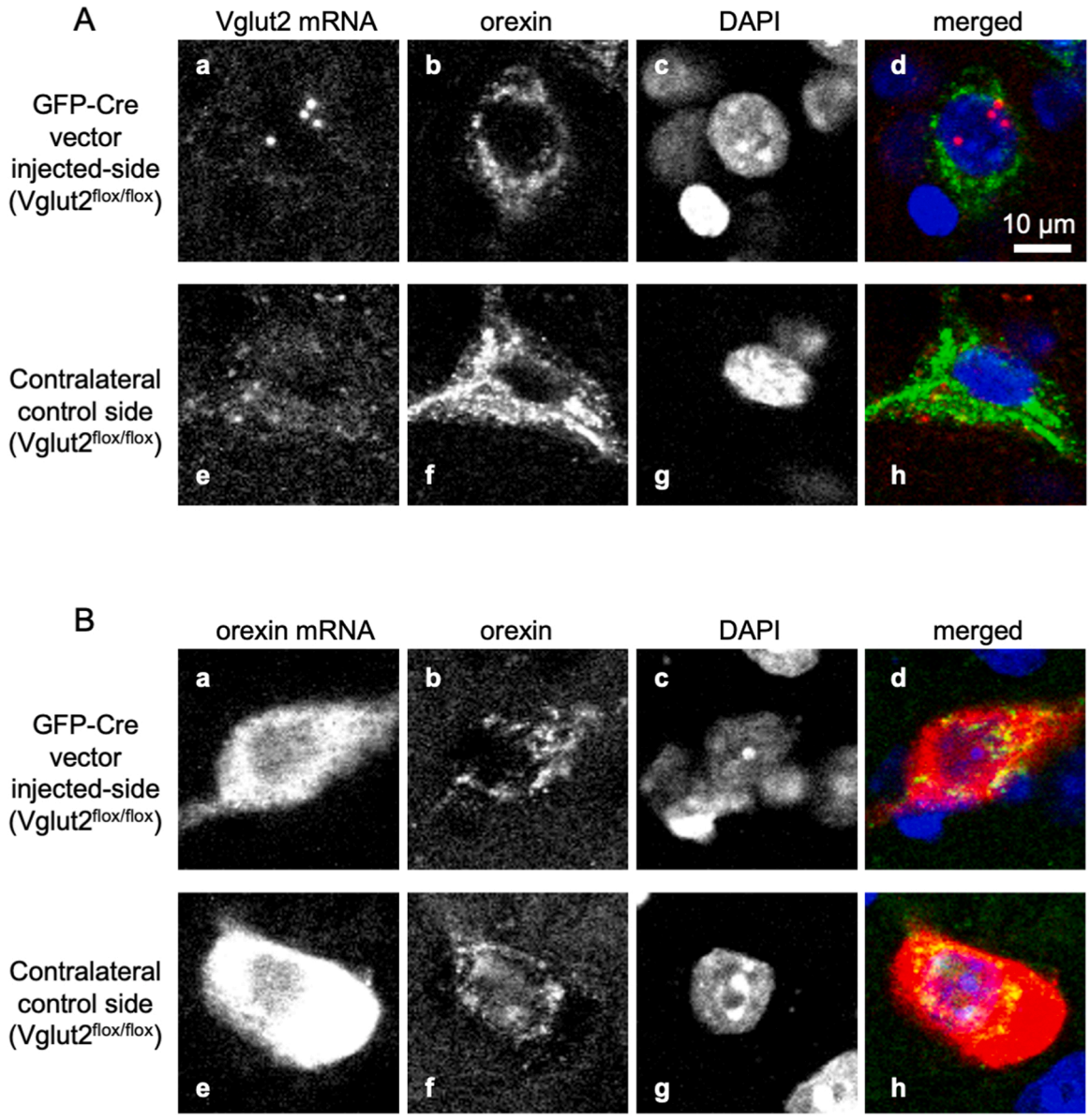


**Fig. 6.** Histochemical analysis showing Cre-driven denaturing specific to the Vglut2 gene.A and B: In Vglut2$^{flox/flox}$ mice with unilateral injection of AAV5-CMV-GFP-Cre into the lateral hypothalamus, a similar intra-nuclear abnormal condensation of Vglut2 mRNA (red in A) was shown in orexin neurons (green in A) in the injection side (A-d) but not in the contralateral side (A-h), while normal orexin mRNA (red in B) without the intra-nuclear abnormal condensation and localization was shown in orexin neurons (green in B) in both injection (B-d) and contralateral sides (B-h). (For interpretation of the references to colour in this figure legend, the reader is referred to the web version of this article.)

METH-induced dose-dependent changes in body temperature with a telemetry probe (Arora et al., 2001; Myles et al., 2008; Phelps et al., 2010; Rusyniak et al., 2012). In the rat study reported by Phelps et al., (Phelps et al., 2010), a significant body temperature increase occurs at 45–60 min for 0.5 m/kg, 90–120 min for 2 mg/kg and 100–240 min for 5 mg/kg. In other words, the effect of METH on body temperature is not dose-dependent, and the latency or patterning of the response varies with dose. In the present mice study, body temperature responses to METH were not dose-dependent either and showed a similar pattern to the rat report. Along with the previous rat work, the present study highlights that the pharmacological effect of METH on body temperature is not uniform and thus must be mediated by complex mechanisms.

Previous studies have suggested that there are two phases of body temperature response to METH. The first phase peaks approximately 60 min after administration, followed by the second phase that peaks at approximately 180 min (Myles et al., 2008). In the first phase, the temperature changes induced by METH can be hypothermic or hyperthermic, suggesting that METH acts on both temperature-increasing and -decreasing mechanisms and that the extent of its action is influenced by the experimental conditions (Myles et al., 2008). In the present study, body temperature decreased to pre-injection levels after a transient increase in the first phase in WT mice. It is therefore likely that METH acts on both thermogenic and hypothermic mechanisms in mice also. Interestingly, the treatment of ORX-KO mice with METH (5 mg/kg) resulted in a hypothermic tendency in the first phase. This result suggests that the hypothermic mechanism is enhanced without orexin in this phase. In rats, orexin-receptor antagonists attenuate hyperthermic responses induced by 5 mg/kg METH (Rusyniak et al., 2012). Thus, orexin neuropeptides appear to play a role in METH-induced hyperthermia, possibly suppressing the hypothermic effects of METH.

In the present study, a low dose of METH (0.5 mg/kg) produced a monophasic increase in body temperature. The magnitude of this

increase in WT and ORX-KO mice was not significantly different from the vehicle control in these two groups, suggesting that 0.5 mg/kg METH did not appear to cause a significant hyperthermic response. Remarkably, this dose of METH did cause a large increase in body temperature in ORX;vGT2-KO mice, and the duration of the hyperthermic response was longer comparing to WT and ORX-KO groups (Fig. 2b). This suggests that METH does actually affect thermoregulatory mechanisms at this low dose. It is plausible that METH may equally act on hyperthermic and hypothermic mechanisms at 0.5 mg/kg in WT and ORX-KO mice, making it appear to have no effect on body temperature. Glutamate from orexin neurons may have an important role in suppressing METH-induced hyperthermia at this dose.

In mice and rats, the main heat-producing organ is brown adipose tissue, and the main heat-dissipating organ is the tail skin. Our previous report demonstrates that methylenedioxymethamphetamine (MDMA), a derivative of METH, increases brown adipose tissue thermogenesis bimodally with the first peak seen within 60 min of administration, followed by a second peak within the next 60 min (Blessing et al., 2006). This report also shows that tail skin blood flow increases (enhanced heat dissipation via vasodilatation) in the first phase and decreases (attenuated heat dissipation via vasoconstriction) in the second phase. The tail skin vasodilation response to METH (0.5 mg/kg) may be supressed in ORX;vGT2-KO mice, which leads to significant hyperthermia in the first phase. In ORX-KO mice, cutaneous vasodilatation may be enhanced with METH (5 mg/kg), leading to hypothermia. Glutamate signalling from orexin neurons may be involved in brain mechanisms mediating the cutaneous vasodilation response to METH, while orexin signalling may contribute to the cutaneous vasoconstriction response. It is necessary to examine the effects of METH on tail skin blood flow in these transgenic mice.

In rat studies, heart rate is increased by a similar dose of METH used in the present study (Arora et al., 2001; Rusyniak et al., 2012; Yoshida et al., 1993). In anesthetized normal mice, 5 mg/kg METH increases heart rate by about 300 bpm (Polesskaya et al., 2011). In contrast to these previous studies, our study found that heart rate was not significantly altered by METH at all doses in WT mice. Interestingly, a low dose of METH (0.5 mg/kg) significantly increased heart rate in ORX;vGT2-KO mice and a high dose of METH (5 mg/kg) decreased heart rate in both ORX-KO and ORX;vGT2-KO mice. In WT controls, the effects of METH on heart rate-increasing and -decreasing mechanisms may be balanced and therefore no significant changes in heart rate were observed. At a low dose of METH, loss of glutamate from orexin neurons may disturb this balance, leading to tachycardia in ORX;vGT2-KO mice. However, orexin may not be involved in mediating this tachycardia, because blockade of orexin-1 receptors does not significantly affect METH-induced tachycardia (Rusyniak et al., 2012). At middle and high doses, METH may act preferentially on heart rate-decreasing mechanism in the absence of glutamate or orexin release from orexin neurons. Since heart rate is under sympathetic and parasympathetic control, it remains to be investigated whether METH-induced bradycardia involves activation of the vagus nerves.

In the present study, METH caused a similar increase in locomotor activity between WT, ORX-KO and ORX;vGT2-KO mice. ORX-KO mice had a lower mean increase in locomotor activity after a high dose of METH compared to WT and ORX;vGT2-KO mice, but differences did not reach the level of statistical significance (Fig. 4). A simple interpretation of this result is that neither orexin nor glutamate from orexin neurons plays a role in METH-induced hyper-locomotor activity. This view is inconsistent as previous reports in which the METH-induced hyperactivity, with the dose of 2 mg/kg, is less in ORX-KO compared to WT mice (Mori et al., 2010). It should be noted that there are several differences in the experimental procedures between the present and previous studies. In the present study, animals were allowed to have a 36-hour habituation time in order to reduce possible psychological stress to a new environment, while animals had only a 90-minute habitation time in the previous study. The experimental room temperature was maintained between 25 and 28°C (the thermoneutral range) to minimise thermoregulatory stress in the present study, whilst a lower temperature range (20–25°C) was used in the previous study. In other words, mice in the previous study were likely under more stress from their environmental conditions. The difference in degree of pre-exposed stress level may explain the result discrepancy.

The previous report (Mori et al., 2010) also used orexin-ataxin3 mice, in which orexin-producing neurons are destroyed genetically (Hara et al., 2001). It was shown that hyper-locomotion induced by 2 mg/kg METH was significantly less in these transgenic mice compared to ORX-KO mice. This data suggests that co-existent neurotransmitters in orexin neurons can play an important role in METH-induced hyperactivity, since the orexin-ataxin3 mice lack both orexin and other neurotransmitters in the orexin neuron. However, glutamate is probably not the candidate as hyper-locomotion was not affected in the ORX;vGT2-KO mice in the present study.

We generated ORX;vGT2-KO mice by crossing orexin-Cre mice (Matsuki et al., 2009) with Vglut2$^{flox/flox}$ mice (Tong et al., 2007). The efficacy of eliminating Vglut2 by Cre-loxP technique using Vglut2$^{flox/flox}$ mice has been demonstrated previously (Abbott et al., 2014; Birgner et al., 2010; Kaur et al., 2013; Roccaro-Waldmeyer et al., 2018; Tong et al., 2007). Since the ORX;vGT2-KO mice have exon 2 of the Vglut2 gene deleted via Cre-induced recombination selectively in orexin neurons, no translation of the exon 2 is assumed in orexin neurons. As expected, the immunohistochemical examination showed that exon 2 mRNA was reduced in the cytoplasm of orexin neurons, while some could be found in the nucleus. We do not know the cause of this intra-nuclei expression. It could be a characteristic of the Vglut2$^{flox/flox}$ line since similar intra-nuclei expression seems to also have occurred in a previous report with this transgenic mice line (Fig. 3D in Kaur et al., 2013). Nevertheless, the reduction of Vglut2 mRNA expression in the cytoplasm of orexin neurons in the ORX;vGT2-KO mice suggests loss of functional vGLUT2 from these neurons.

Orexin neurons express vGLUT2 predominantly over vGLUT1 (Rosin et al., 2003), suggesting that vGLUT2 is the main contributor to glutamate release from orexin neurons. Eliminating vGLUT2-dependent glutamatergic neurotransmission with the Vglut2$^{flox/flox}$ mice line has been previously confirmed in vGLUT2-deleted neurons that express steroidogenic factor 1 in the hypothalamus (Tong et al., 2007) or in dopamine neurons in the midbrain (Shen et al., 2018). It is assumed that in the ORX;vGT2-KO mice, deletion of vGLUT2 leads to loss of glutamate release from orexin neurons. This point will need to be confirmed in future in vitro studies.

In a study that selectively deleted vGLUT2 in tyrosine hydroxylase-synthesizing neurons, the morphology and projection pattern of these neurons are not altered (Abbott et al., 2014), suggesting that glutamate release via vGLUT2 is not crucial for their development. In the present study, no notable changes in morphology and orexin expression were observed in the orexin neurons ORX;vGT2-KO mice upon visual inspection, suggesting that the loss of vGLUT2 does not affect the development of orexin neurons.

It has been suggested that vGLUT2 may function in the vesicular filling of catecholamines in dopaminergic neurons in the midbrain (Hnasko et al., 2010). If a similar vesicular filling mechanism for neurotransmitters exist in orexin neurons that co-express vGLUT2, release of orexin and other co-transmitters may be affected in ORX;vGT2-KO mice. Furthermore, loss of glutamate transmission due to vGLUT2 deficiency may cause compensatory changes in the postsynaptic receptor expression for orexin and other co-transmitters. The consideration of such possibilities will be the subject of a future issue.

Studies using c-Fos have shown that METH activates orexin neurons (Estabrooke et al., 2001). Our findings that METH-induced changes in body temperature and heart rate varied depending on genotype and dose point to non-uniform activation of orexin neurons. Indeed, not all orexin neurons express c-Fos after administration of amphetamine, the parent compound of METH (Fadel et al., 2002). This suggests that orexin

neurons are not a functionally homogenous entity (Fadel et al., 2002). In support of this view, not all orexin neurons express glutamate – with it being expressed in only about 50% of orexin neurons (Rosin et al., 2003). Low concentrations of METH may selectively activate glutamate-expressing orexin neurons, while high concentrations of METH might also involve other orexin neurons. Further studies are required to clarify these points.

It has been suggested that glutamate and orexin co-released from orexin neurons have different effects on descending neurons in in-vitro studies (Schone et al., 2014). Our experiment suggests, for the first time, that orexin peptides and glutamate released from orexin neurons have a differential role in mediating body temperature and heart rate responses to METH. Deficiency of Vglut 2 gene in the orexin neurons enhances hyperthermic and tachycardic responses to METH suggesting that glutamate has a mitigating effect on METH excitatory action on thermoregulatory and cardiovascular function. Loss of the orexin peptide exaggerates hypothermic and bradycardic responses to METH suggesting that orexin has a suppressive action on METH inhibitory actions. The present study indicates that the role orexin neurons play in METH-induced body temperature and heart rate response is multifaceted.

Orexin transmission requires a higher level of presynaptic activity than glutamate transmission, suggesting that the two transmissions are independent (Schone et al., 2014) and that they do not necessarily occur in the same nerve terminal at the same time. It is also possible that glutamate and orexin from orexin neurons act on different downstream neuronal circuits, as vGLUT2 is not expressed in all orexin neurons (Blanco-Centurion et al., 2018; Rosin et al., 2003). Glutamate can be an inhibitory neurotransmitter (Fiorillo and Williams, 1998; Grueter and Winder, 2005). Therefore, the effects of orexin and glutamate on the final outputs could be opposite.

## Acknowledgements

The authors thank Ms Miki Sakoda at Kagoshima University and members of the Fukazawa laboratory and Life Science Research Laboratory at University of Fukui for technical assistance. We also thank Anna Antipov and Jett Zivkovic from Flinders University for proof reading. This research was supported by the Japan Society for the Promotion of Science KAKENHI Grant Number 23590280 to YO and 24390057 to TK, Japan and by Kodama Memorial Foundation for Medical Research to YO, Japan. Ootsuka and Kuwaki designed the research. Miyata, Ikoma and Ootsuka performed and analyzed all physiological recordings from animals. Murata, Kusumoto-Yoshida and Kobayashi performed the in situ hybridization experiment and its histological analysis. Miyata and Ootsuka drafted the manuscript. Miyata, Kuwaki and Ootsuka revised the manuscript. All authors have approved the final version of the manuscript and agreed to be accountable for all aspects of the work.

### *CRediT authorship contribution statement*

This research was supported by the Japan Society for the Promotion of Science (KAKENHI) (23590280 to YO and 24390057 to TK) and by Kodama Memorial Foundation for Medical Research to YO. Ootsuka and Kuwaki designed the research. Miyata, Ikoma and Ootsuka performed and analyzed all physiological recordings from animals. Murata, Kusumoto-Yoshida and Kobayashi performed the in situ hybridization experiment and its histological analysis. Miyata and Ootsuka drafted the manuscript. Miyata, Kuwaki and Ootsuka revised the manuscript. All authors have approved the final version of the manuscript and agreed to be accountable for all aspects of the work.

## References

Abbott, S.B.G., Holloway, B.B., Viar, K.E., Guyenet, P.G., 2014. Vesicular glutamate transporter 2 is required for the respiratory and parasympathetic activation produced by optogenetic stimulation of catecholaminergic neurons in the rostral ventrolateral medulla of mice in vivo. Eur. J. Neurosci. 39, 98–106.

Anneken, J.H., Angoa-Perez, M., Sati, G.C., Crich, D., Kuhn, D.M., 2018. Assessing the role of dopamine in the differential neurotoxicity patterns of methamphetamine, mephedrone, methcathinone and 4-methylmethamphetamine. Neuropharmacology 134, 46–56.

Arora, H., Owens, S.M., Brooks, Gentry, W., 2001. Intravenous (+)-methamphetamine causes complex dose-dependent physiologic changes in awake rats. Eur. .J Pharmacol. 426, 81–87.

Behrouzvaziri, A., Fu, D., Tan, P., Yoo, Y., Zaretskaia, M.V., Rusyniak, D.E., Molkov, Y.I., Zaretsky, D.V., 2015. Orexinergic neurotransmission in temperature responses to methamphetamine and stress: mathematical modeling as a data assimilation approach. PLoS One 10, e0126719.

Birgner, C., Nordenankar, K., Lundblad, M., Mendez, J.A., Smith, C., le Greves, M., Galter, D., Olson, L., Fredriksson, A., Trudeau, L.E., Kullander, K., Wallen-Mackenzie, A., 2010. VGLUT2 in dopamine neurons is required for psychostimulant-induced behavioral activation. Proc Natl. Acad. Sci. U S A 107, 389–394.

Blanco-Centurion, C., Bendell, E., Zou, B., Sun, Y., Shiromani, P.J., Liu, M., 2018. VGAT and VGLUT2 expression in MCH and orexin neurons in double transgenic reporter mice. IBRO Reports 4, 44–49.

Blessing, W.W., Zilm, A., Ootsuka, Y., 2006. Clozapine reverses increased brown adipose tissue thermogenesis induced by 3,4-methylenedioxymethamphetamine and by cold exposure in conscious rats. Neuroscience 141, 2067–2073.

Chemelli, R.M., Willie, J.T., Sinton, C.M., Elmquist, J.K., Scammell, T., Lee, C., Richardson, J.A., Williams, S.C., Xiong, Y., Kisanuki, Y., Fitch, T.E., Nakazato, M., Hammer, R.E., Saper, C.B., Yanagisawa, M., 1999. Narcolepsy in orexin knockout mice: molecular genetics of sleep regulation. Cell 98, 437–451.

DiMicco, J.A., Sarkar, S., Zaretskaia, M.V., Zaretsky, D.V., 2006. Stress-induced cardiac stimulation and fever: common hypothalamic origins and brainstem mechanisms. Auton Neurosci 126–127, 106–119.

Dimicco, J.A., Zaretsky, D.V., 2007. The dorsomedial hypothalamus: a new player in thermoregulation. Am. J. Physiol. Regul. Integr. Comp. Physiol. 292, R47–R63.

El Mestikawy, S., Wallén-Mackenzie, Å., Fortin, G.M., Descarries, L., Trudeau, L.-E., 2011. From glutamate co-release to vesicular synergy: vesicular glutamate transporters. Nature Rev. Neurosci. 12, 204–216.

Estabrooke, I.V., McCarthy, M.T., Ko, E., Chou, T.C., Chemelli, R.M., Yanagisawa, M., Saper, C.B., Scammell, T.E., 2001. Fos expression in orexin neurons varies with behavioral state. J. Neurosci. 21, 1656–1662.

Fadel, J., Bubser, M., Deutch, A.Y., 2002. Differential activation of orexin neurons by antipsychotic drugs associated with weight gain. J. Neurosci.: Official J. Soc. Neurosci. 22, 6742–6746.

Fantegrossi, W.E., Ciullo, J.R., Wakabayashi, K.T., De La Garza, R., 2nd, Traynor, J.R., Woods, J.H., 2008. A comparison of the physiological, behavioral, neurochemical and microglial effects of methamphetamine and 3,4-methylenedioxymethamphetamine in the mouse. Neuroscience 151, 533–543.

Fiorillo, C.D., Williams, J.T., 1998. Glutamate mediates an inhibitory postsynaptic potential in dopamine neurons. Nature 394, 78–82.

Funahashi, M., Kohda, H., Hori, O., Hayashida, H., Kimura, H., 1990. Potentiating effect of morphine upon d-methamphetamine-induced hyperthermia in mice. Effects of naloxone and haloperidol. Pharmacol. Biochem. Behav. 36, 345–350.

Funahashi, M., Kohda, H., Shikata, I., Kimura, H., 1988. Potentiation of lethality and increase in body temperature by combined use of d-methamphetamine and morphine in mice. Forensic. Sci. Int. 37, 19–26.

Grueter, B.A., Winder, D.G., 2005. Group II and III metabotropic glutamate receptors suppress excitatory synaptic transmission in the dorsolateral bed nucleus of the stria terminalis. Neuropsychopharmacology 30, 1302–1311.

Hara, J., Beuckmann, C.T., Nambu, T., Willie, J.T., Chemelli, R.M., Sinton, C.M., Sugiyama, F., Yagami, K., Goto, K., Yanagisawa, M., Sakurai, T., 2001. Genetic ablation of orexin neurons in mice results in narcolepsy, hypophagia, and obesity. Neuron 30, 345–354.

Hnasko, T.S., Chuhma, N., Zhang, H., Goh, G.Y., Sulzer, D., Palmiter, R.D., Rayport, S., Edwards, R.H., 2010. Vesicular glutamate transport promotes dopamine storage and glutamate corelease in vivo. Neuron 65, 643–656.

Kaspar, B.K., Vissel, B., Bengoechea, T., Crone, S., Randolph-Moore, L., Muller, R., Brandon, E.P., Schaffer, D., Verma, I.M., Lee, K.F., Heinemann, S.F., Gage, F.H., 2002. Adeno-associated virus effectively mediates conditional gene modification in the brain. Proc. Natl. Acad. Sci. U S A 99, 2320–2325.

Kataoka, N., Hioki, H., Kaneko, T., Nakamura, K., 2014. Psychological stress activates a dorsomedial hypothalamus-medullary raphe circuit driving brown adipose tissue thermogenesis and hyperthermia. Cell Metab. 20, 346–358.

Kataoka, N., Shima, Y., Nakajima, K., Nakamura, K., 2020. A central master driver of psychosocial stress responses in the rat. Science 367, 1105–1112.

Kaur, S., Pedersen, N.P., Yokota, S., Hur, E.E., Fuller, P.M., Lazarus, M., Chamberlin, N. L., Saper, C.B., 2013. Glutamatergic signaling from the parabrachial nucleus plays a critical role in hypercapnic arousal. J. Neurosci. 33, 7627.

Kaushal, N., Seminerio, M.J., Shaikh, J., Medina, M.A., Mesangeau, C., Wilson, L.L., McCurdy, C.R., Matsumoto, R.R., 2011. CM156, a high affinity sigma ligand, attenuates the stimulant and neurotoxic effects of methamphetamine in mice. Neuropharmacology 61, 992–1000.

Kayaba, Y., Nakamura, A., Kasuya, Y., Ohuchi, T., Yanagisawa, M., Komuro, I., Fukuda, Y., Kuwaki, T., 2003. Attenuated defense response and low basal blood

pressure in orexin knockout mice. Am. J. Physiol. Regul. Integr. Comp. Physiol. 285, R581–R593.
Kobayashi, K., Sano, H., Kato, S., Kuroda, K., Nakamuta, S., Isa, T., Nambu, A., Kaibuchi, K., Kobayashi, K., 2016. Survival of corticostriatal neurons by Rho/Rho-kinase signaling pathway. Neurosci. Lett. 630, 45–52.
Kuwaki, T., 2015. Thermoregulation under pressure: a role for orexin neurons. Temperature 2, 379–391.
Kuwaki, T., Zhang, W., 2012. Orexin neurons and emotional stress. Vitam. Horm. 89, 135–158.
Matsuki, T., Nomiyama, M., Takahira, H., Hirashima, N., Kunita, S., Takahashi, S., Yagami, K.-i, Kilduff, T.S., Bettler, B., Yanagisawa, M., Sakurai, T., 2009. Selective loss of GABAB receptors in orexin-producing neurons results in disrupted sleep/wakefulness architecture. Proceedings of the National Academy of Sciences 106, 4459–4464.
Mori, T., Ito, S., Kuwaki, T., Yanagisawa, M., Sakurai, T., Sawaguchi, T., 2010. Monoaminergic neuronal changes in orexin deficient mice. Neuropharmacology 58, 826–832.
Murata, K., Kinoshita, T., Ishikawa, T., Kuroda, K., Hoshi, M., Fukazawa, Y., 2020. Region- and neuronal-subtype-specific expression of Na,K-ATPase alpha and beta subunit isoforms in the mouse brain. J. Comp. Neurol. 528, 2654–2678.
Myles, B.J., Jarrett, L.A., Broom, S.L., Speaker, H.A., Sabol, K.E., 2008. The effects of methamphetamine on core body temperature in the rat–part 1: chronic treatment and ambient temperature. Psychopharmacology 198, 301–311.
Namiki, M., Mori, T., Sawaguchi, T., Ito, S., Suzuki, T., 2005. Underlying mechanism of combined effect of methamphetamine and morphine on lethality in mice and therapeutic potential of cooling. J. Pharmacol. Sci. 99, 168–176.
Phelps, G., Speaker, H.A., Sabol, K.E., 2010. Relationship between methamphetamine-induced behavioral activation and hyperthermia. Brain Res. 1357, 41–52.
Polesskaya, O., Silva, J., Sanfilippo, C., Desrosiers, T., Sun, A., Shen, J., Feng, C., Polesskiy, A., Deane, R., Zlokovic, B., Kasischke, K., Dewhurst, S., 2011. Methamphetamine causes sustained depression in cerebral blood flow. Brain Res. 1373, 91–100.
Roccaro-Waldmeyer, D.M., Girard, F., Milani, D., Vannoni, E., Prétôt, L., Wolfer, D.P., Celio, M.R., 2018. Eliminating the VGlut2-dependent glutamatergic transmission of parvalbumin-expressing neurons leads to deficits in locomotion and vocalization, decreased pain sensitivity, and increased dominance. Front. Behav. Neurosci. 12.
Rosin, D.L., Weston, M.C., Sevigny, C.P., Stornetta, R.L., Guyenet, P.G., 2003. Hypothalamic orexin (hypocretin) neurons express vesicular glutamate transporters VGLUT1 or VGLUT2. J. Comp. Neurol. 465, 593–603.
Rusyniak, D.E., Zaretskaia, M.V., Zaretsky, D.V., DiMicco, J.A., 2008. Microinjection of muscimol into the dorsomedial hypothalamus suppresses MDMA-evoked sympathetic and behavioral responses. Brain Res. 1226, 116–123.
Rusyniak, D.E., Zaretsky, D.V., Zaretskaia, M.V., Durant, P.J., DiMicco, J.A., 2012. The orexin-1 receptor antagonist SB-334867 decreases sympathetic responses to a moderate dose of methamphetamine and stress. Physiol. Behav. 107, 743–750.
Sakurai, T., 2007. The neural circuit of orexin (hypocretin): maintaining sleep and wakefulness. Nat. Rev. Neurosci. 8, 171–181.
Schone, C., Apergis-Schoute, J., Sakurai, T., Adamantidis, A., Burdakov, D., 2014. Coreleased orexin and glutamate evoke nonredundant spike outputs and computations in histamine neurons. Cell reports 7, 697–704.
Shen, H., Marino, R.A.M., McDevitt, R.A., Bi, G.-H., Chen, K., Madeo, G., Lee, P.-T., Liang, Y., De Biase, L.M., Su, T.-P., Xi, Z.-X., Bonci, A., 2018. Genetic deletion of vesicular glutamate transporter in dopamine neurons increases vulnerability to MPTP-induced neurotoxicity in mice. Proceedings of the National Academy of Sciences 115, E11532.
Takahashi, Y., Zhang, W., Sameshima, K., Kuroki, C., Matsumoto, A., Sunanaga, J., Kono, Y., Sakurai, T., Kanmura, Y., Kuwaki, T., 2013. Orexin neurons are indispensable for prostaglandin E2-induced fever and defence against environmental cooling in mice. J. Physiol. 591, 5623–5643.
Tong, Q., Ye, C., McCrimmon, R.J., Dhillon, H., Choi, B., Kramer, M.D., Yu, J., Yang, Z., Christiansen, L.M., Lee, C.E., Choi, C.S., Zigman, J.M., Shulman, G.I., Sherwin, R.S., Elmquist, J.K., Lowell, B.B., 2007. Synaptic glutamate release by ventromedial hypothalamic neurons is part of the neurocircuitry that prevents hypoglycemia. Cell Metab. 5, 383–393.
Torrealba, F., Yanagisawa, M., Saper, C.B., 2003. Colocalization of orexin a and glutamate immunoreactivity in axon terminals in the tuberomammillary nucleus in rats. Neuroscience 119, 1033–1044.
Tsujino, N., Sakurai, T., 2009. Orexin/hypocretin: a neuropeptide at the interface of sleep, energy homeostasis, and reward system. Pharmacol. Rev. 61, 162–176.
Watakabe, A., Komatsu, Y., Ohsawa, S., Yamamori, T., 2010. Fluorescent in situ hybridization technique for cell type identification and characterization in the central nervous system. Methods 52, 367–374.
Yoshida, K., Morimoto, A., Makisumi, T., Murakami, N., 1993. Cardiovascular, thermal and behavioral sensitization to methamphetamine in freely moving rats. J. Pharmacol. Exp. Ther. 267, 1538–1543.
Zhang, W., Shimoyama, M., Fukuda, Y., Kuwaki, T., 2006. Multiple components of the defense response depend on orexin: evidence from orexin knockout mice and orexin neuron-ablated mice. Auton Neurosci. 126–127, 139–145.
Zhang, W., Sunanaga, J., Takahashi, Y., Mori, T., Sakurai, T., Kanmura, Y., Kuwaki, T., 2010. Orexin neurons are indispensable for stress-induced thermogenesis in mice. J. Physiol. 588, 4117–4129.